CHINESE OPTICS LETTERS

Vol. 19, No. 3 | March 2021

High-brightness red-emitting double-perovskite phosphor $Sr_2LaTaO_6:Eu^{3+}$ with high color purity and thermal stability [Invited]

Zongjie Zhang (张宗杰), Wei Li (李 伟), Nan Ma (马 楠), and Xiaoyong Huang (黄小勇)*

College of Physics and Optoelectronics, Taiyuan University of Technology, Taiyuan 030024, China

*Corresponding author: huangxy04@126.com

Received December 16, 2020 | Accepted January 12, 2021 | Posted Online February 8, 2021

Bright Eu^{3+}-activated double-perovskite Sr_2LaTaO_6 red-emitting phosphors were successfully synthesized by a high-temperature solid-state method. Under near-ultraviolet excitation at 394 nm, optimal $Sr_2LaTaO_6:0.2Eu^{3+}$ phosphors emitted high-brightness red light around 613 nm with the International Commission on Illumination chromaticity coordinates (0.650, 0.349). Notably, the color purity can reach 92%. Impressively, the favorable thermal stability of the $Sr_2LaTaO_6:0.2Eu^{3+}$ phosphors was characterized by temperature-dependent emission spectra at different temperatures from 303 to 463 K, and the emission intensity at 423 K remained 73% of its value at 303 K. All of the results suggested that the as-prepared $Sr_2LaTaO_6:0.2Eu^{3+}$ phosphors can be used in near-ultraviolet-excitable white light-emitting diodes as a red-emitting color converter.

Keywords: Sr_2LaTaO_6; Eu^{3+}; double-perovskite; phosphors.

DOI: 10.3788/COL202119.030003

1. Introduction

Due to excellent energy efficiency, long service life, and environmental friendliness, white light-emitting diodes (LEDs) are considered to be the next-generation illumination solution[1–5]. Nowadays, the widely used white LEDs are commonly manufactured by combining InGaN blue LED chips with $Y_3Al_5O_{12}:Ce^{3+}$ yellow-emitting phosphors[6]. However, due to the lack of red light, there are some limitations in these white LEDs, including highly correlated color temperature (CCT) and low color rendering index (CRI)[7]. At present, the near-ultraviolet (UV) LED chips coated with tri-color (blue, green, and red) phosphors are proposed as a promising way to fabricate white LEDs[8–10]. Thus, research on near-UV-light-excitable red phosphor is a very meaningful work.

The Eu^{3+} ion is a superior rare-earth ion to achieve red light emission[11–14]. As a host material, a double-perovskite compound with molecular formula A_2BMO_6 is a wise choice for the luminescence field[15]. Phosphors based on double-perovskite compounds could show excellent chemical and physical stability and outstanding optical characteristics.

To the best of our knowledge, no publication has reported on Eu^{3+} ion-doped Sr_2LaTaO_6 (abbreviated as SLT) double-perovskite so far. Herein, we reported on the synthesis and luminescent properties of Eu^{3+}-activated SLT red-emitting phosphors. Single-phase SLT:Eu^{3+} phosphors were prepared by the conventional high-temperature solid-state reaction method. These phosphors showed an excitation peak around 394 nm, which matched well with the emission wavelength of near-UV LED chips. Upon excitation at 394 nm, bright red emissions around 613 nm were observed, along with high color purity of 92%. The resistance to luminescence thermal quenching at high temperatures was also studied.

2. Experimental Section

2.1. Synthesis of the samples

The SLT host and SLT:xEu^{3+} ($x = 0.1$, 0.15, 0.2, 0.25, and 0.3) phosphors were synthesized by the high-temperature solid-state reaction route. $SrCO_3$ (99%, Aladdin Industrial Corporation, Shanghai, China), La_2O_3 (99.99%, Jining Tianyi New Materials Co., Ltd.), Ta_2O_5 (99.5%, Aladdin Industrial Corporation, Shanghai, China), and Eu_2O_3 (99.99%, Jining Tianyi New Materials Co., Ltd.) were used as the starting materials, and stoichiometric amounts of these chemicals were weighed. Afterward, the mixtures were thoroughly ground by an agate mortar. The resulting mixtures were put into the alumina crucibles and then heated at 600°C for 3 h and 1500°C for 6 h.

2.2. Characterization

The phase formation of the SLT:0.2Eu^{3+} phosphors and SLT host was investigated by powder X-ray diffraction (PXRD) with Cu Kα ($\lambda = 1.5406$ Å, 1 Å = 0.1 nm) radiation. Then, the photoluminescence excitation (PLE) and photoluminescence (PL) spectra and decay curves were measured by an Edinburgh FS5 spectrometer with the 150 W xenon lamp and the pulsed xenon lamp as the light source, respectively. Eventually, the temperature-dependent PL spectra of SLT:0.2Eu^{3+} phosphors were recorded by the same spectrometer connected with a temperature controller (TAP-02).

3. Results and Discussion

3.1. Phase purity

To confirm the phase purity of the as-prepared phosphors, Fig. 1(a) shows the PXRD patterns of the SLT host and SLT:0.2Eu^{3+} phosphors. All of the PXRD peaks of these two samples match well with the standard power diffraction file (PDF) card (PDF #11-0574) of the SLT compound, which indicated that the crystal structure of the as-prepared phosphors did not change after Eu^{3+} doping. As shown in Fig. 1(b), compared with the pure SLT host, the diffraction peak of the SLT:0.2Eu^{3+} sample shifted to a larger angle. This phenomenon can be as attributed to the fact that in SLT:0.2Eu^{3+} phosphors the smaller Eu^{3+} ion [$r = 0.95$ Å, coordination number (CN) = 6] replaced the larger La^{3+} ion ($r = 1.03$ Å, CN = 6)[16,17].

3.2. Photoluminescence properties

The PLE and PL spectra of SLT:0.2Eu^{3+} phosphors are given in Fig. 2(a). It is clear to see that the strongest peaks of the excitation and emission bands were located at 394 and 613 nm, respectively. When monitored at the 613 nm emission, the obtained PLE spectrum of SLT:0.2Eu^{3+} phosphors mainly contained a broad excitation band in the 250–315 nm wavelength range and a group of sharp excitation peaks in the 325–500 nm spectral range. The former broad band originated from the O^{2-} → Eu^{3+} charge transfer band (CTB). The latter sharp PLE peaks were

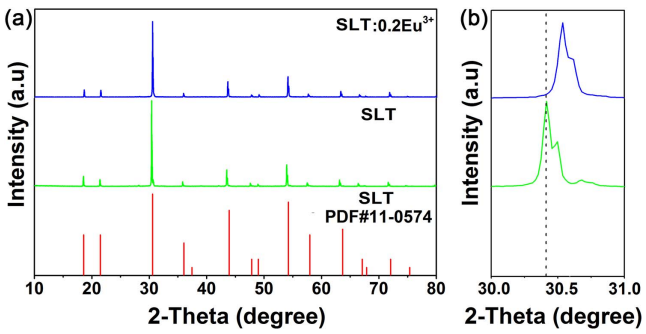

Fig. 1. PXRD patterns of the SLT:0.2Eu^{3+} phosphors and SLT host, in the range of (a) 10–80 deg and (b) 30–31 deg.

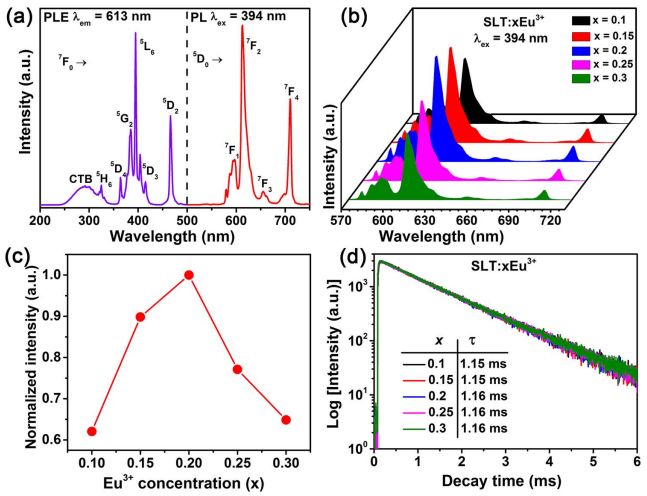

Fig. 2. (a) PLE and PL spectra of the SLT:0.2Eu^{3+} phosphors. (b) PL spectra of the SLT:xEu^{3+} ($x = 0.1$, 0.15, 0.2, 0.25, and 0.3) phosphors. (c) The line chart for PL integrated intensity and Eu^{3+} doping concentration. (d) Decay curves for SLT:xEu^{3+} phosphors.

ascribed to the 4f-4f transitions of Eu^{3+} ions, namely, 325 nm ($^7F_0 \rightarrow {}^5H_6$ transition), 364 nm ($^7F_0 \rightarrow {}^5D_4$ transition), 385 nm ($^7F_0 \rightarrow {}^5G_2$ transition), 394 nm ($^7F_0 \rightarrow {}^5L_6$ transition), 415 nm ($^7F_0 \rightarrow {}^5D_3$ transition), and 466 nm ($^7F_0 \rightarrow {}^5D_2$ transition)[18–20]. Under 394 nm excitation, the SLT:0.2Eu^{3+} phosphors exhibited bright red light. The PL spectrum consisted of several typical sharp emission peaks at 595, 613, 656, and 710 nm, which were attributed to the $^5D_0 \rightarrow {}^7F_1$, $^5D_0 \rightarrow {}^7F_2$, $^5D_0 \rightarrow {}^7F_3$, and $^5D_0 \rightarrow {}^7F_4$ transitions, respectively[21].

Figure 2(b) shows the PL spectra of SLT:xEu^{3+} ($x = 0.1$, 0.15, 0.2, 0.25, and 0.3) phosphors under 394 nm excitation. It can be seen that all of these emission spectra exhibited similar profiles, and the strongest PL intensity was achieved at $x = 0.2$. Figure 2(c) displays the change trend of the integral emission intensity of SLT:xEu^{3+} phosphors with different Eu^{3+} doping concentrations. As can be seen, the optimal doping concentration of Eu^{3+} ions was 20% (mole fraction). When x was higher than 0.2, the emission intensity gradually reduced with increasing Eu^{3+} concentration, due to the concentration quenching effect. The observed concentration quenching was attributed to the energy transfer among nearby Eu^{3+} ions[22].

Luminescence decay curves ($\lambda_{ex} = 394$ nm, $\lambda_{em} = 615$ nm) for SLT:xEu^{3+} phosphors are shown in Fig. 2(d). The lifetimes can be fitted using a single exponential function[23]:

$$I_t = I_0 \exp(-t/\tau), \tag{1}$$

where I_t and I_0 refer to the luminescence intensities of SLT:xEu^{3+} phosphors at time t and zero, and τ represents the decay lifetime. The values of decay lifetime for SLT:xEu^{3+} samples are listed in Fig. 2(d). The values of decay lifetimes were around 1 ms, which were similar to the reported Eu^{3+}-activated phosphors, such as Y_2MoSiO_8:Eu^{3+} ($\tau = 1.06$ ms)[22] and $Sr_{0.95}Al_2Si_2O_8$:0.05Eu^{3+} ($\tau = 1.31$ ms)[11].

The PL spectra of the as-prepared SLT:0.2Eu^{3+} phosphors and commercial Y_2O_2S:Eu^{3+} red phosphors are shown in Fig. 3(a). Upon 394 nm excitation, the integrated emission intensity of SLT:0.2Eu^{3+} phosphors was about three times higher than that of commercial Y_2O_2S:Eu^{3+} red phosphors. To better understand the luminescence mechanism of as-prepared SLT:0.2Eu^{3+} phosphors, the corresponding energy level diagram is illustrated in Fig. 3(b).

The asymmetry ratio (R/O), which is determined as the intensity ratio of red emission ($^5D_0 \rightarrow {}^7F_2$ transition) to orange emission ($^5D_0 \rightarrow {}^7F_4$ transition), can be used to characterize the centrosymmetric geometry of the Eu^{3+} activator. As shown as Fig. 3(c), all of the R/O values of SLT:Eu^{3+} samples were calculated in the range from 2.6 to 2.8. The calculated result illustrated that the Eu^{3+} dopants occupied the asymmetric sites, which was good for high color purity. Figure 3(d) shows the International Commission on Illumination (CIE) chromaticity diagram ($\lambda_{ex} = 394$ nm) and the photograph (under a 365 nm lamp) of SLT:0.2Eu^{3+} phosphors. Clearly, the SLT:0.2Eu^{3+} phosphors emitted bright red light under the 365 nm UV lamp. The CIE chromaticity coordinates of SLT:0.2Eu^{3+} phosphors were determined to be (0.650, 0.349), which were much closer to that of ideal red light (0.67, 0.33). The color purity is an important property for phosphor. The value of color purity can be obtained by the following equation[24]:

$$\text{Color purity} = \frac{\sqrt{(x-x_i)^2+(y-y_i)^2}}{\sqrt{(x_d-x_i)^2+(y_d-y_i)^2}} \times 100\%, \quad (2)$$

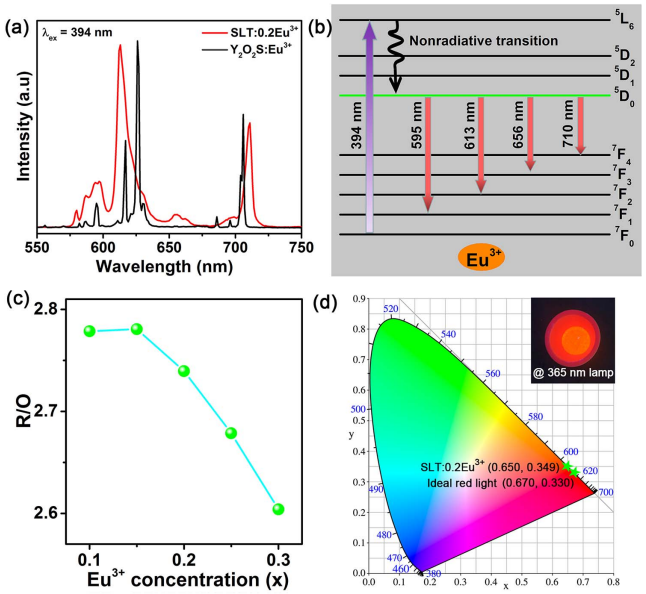

Fig. 3. (a) PL spectra of the as-prepared SLT:0.2Eu^{3+} phosphors and commercial Y_2O_2S:Eu^{3+} red phosphors. (b) Schematic illustration of Eu^{3+} ions energy level in SLT:Eu^{3+} phosphors. (c) The asymmetry ratio as a function of Eu^{3+} doping concentration in SLT:Eu^{3+} phosphors upon 394 nm excitation. (d) CIE chromaticity diagram for SLT:0.2Eu^{3+} phosphors ($\lambda_{ex} = 394$ nm). The inset shows the digital photograph of SLT:0.2Eu^{3+} phosphors under a 365 nm lamp.

where (x, y), (x_d, y_d), and (x_i, y_i) are the CIE coordinates of samples, corresponding to the dominating wavelength and white light, respectively. For the SLT:0.2Eu^{3+} sample, the values of (x, y), (x_d, y_d), and (x_i, y_i) were (0.650, 0.349), (0.682, 0.318), and (0.310, 0.316). The value of the color purity was calculated to be 92%, which was higher than that of $Na_3Sc_2(PO_4)_3$:Eu^{3+} (color purity: 87%)[25] and $Ba_2MgGe_2O_7$:Eu^{3+} (color purity: 90%)[26].

3.3. Thermal stability

Figure 4(a) shows the temperature-dependent PL spectra of SLT:0.2Eu^{3+} phosphors. With the temperature increasing from 303 K to 463 K, the PL intensity gradually decreased. The temperature-dependent normalized integrated PL intensity is depicted in Fig. 4(b). When the temperature of the SLT:0.2Eu^{3+} sample was 423 K, the emission intensity of the sample still reserved 73% of the intensity at 303 K. For further comprehending the thermal quenching behavior, the activation energy (E_a) can be calculated by Arrhenius equation[27]:

$$\ln\left(\frac{I_0}{I}-1\right) = \ln A - \frac{E_a}{kT}, \quad (3)$$

where I_0 is the initial emission intensity, I is the intensity at temperature T, A is a constant, and k is the Boltzmann constant. As shown in Fig. 4(c), the slope of $\ln(I_0/I-1)$ versus $1/kT$ (eV^{-1}) was −0.26, which meant that the value of the E_a was 0.26 eV. The thermal quenching process of Eu^{3+} ions in SLT:Eu^{3+} phosphors is illustrated in Fig. 4(d).

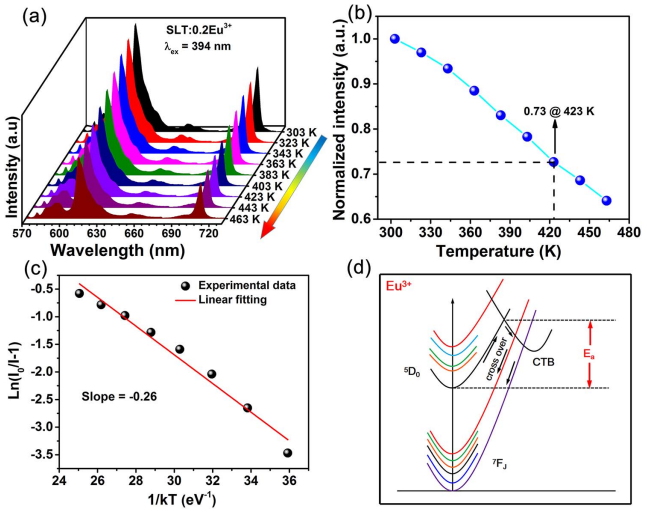

Fig. 4. (a) PL spectra of the SLT:0.2Eu^{3+} phosphors at different temperature from 303 to 463 K. (b) Normalized integrated temperature-dependent PL intensity in wavelength range of 550–750 nm. (c) Fitting plot of ln (I_0/I-1) versus $1/kT$ for SLT:Eu^{3+} phosphors. (d) Configuration diagram of the ground and excited states for Eu^{3+} ions in SLT:Eu^{3+} phosphors.

4. Conclusion

In this work, highly luminescent SLT:Eu^{3+} red phosphors have been prepared by using a facile high-temperature solid-state approach. The PXRD certified that phosphors with pure phase were prepared. The optimal doping concentration of Eu^{3+} ions was $x = 0.2$. Upon 394 nm excitation, the intensity of SLT:$0.2Eu^{3+}$ phosphors was about three times as great as commercial Y_2O_2S:Eu^{3+} red phosphors. Notably, the CIE chromaticity coordinates of SLT:$0.2Eu^{3+}$ phosphors were (0.650, 0.349), and the color purity can reach as high as 92%. Besides, E_a was obtained as 0.26 eV, and the emission intensity of SLT:$0.2Eu^{3+}$ phosphors at 423 K was 73% of that at 303 K. These results suggested that the as-prepared SLT:Eu^{3+} red phosphors can be used as color converter in near-UV-pumped white LEDs.

Acknowledgement

This work was supported by the National Natural Science Foundation of China (No. 51502190), Young Sanjin Scholars Distinguished Professor Program of Shanxi Province, Open Fund of the State Key Laboratory of Luminescent Materials and Devices (South China University of Technology, No. 2020-skllmd-01), and Graduate Education Innovation Project of Shanxi Province.

References

1. J. Si, L. Wang, L. Liu, W. Yi, G. Cai, T. Takeda, S. Funahashi, N. Hirosaki, and R.-J. Xie, "Structure, luminescence and energy transfer in Ce^{3+} and Mn^{2+} codoped γ-AlON phosphors," J. Mater. Chem. C **7**, 733 (2019).
2. D. Wen, H. Kato, and M. Kakihana, "Super stable (Ba,Sr)$LuAl_2Si_2O_2N_5$:Ce^{3+}, Eu^{2+} phosphors," J. Mater. Chem. C **8**, 4510 (2020).
3. J. Liang, B. Devakumar, L. Sun, S. Wang, Q. Sun, and X. Huang, "Full-visible-spectrum lighting enabled by an excellent cyan-emitting garnet phosphor," J. Mater. Chem. C **8**, 4934 (2020).
4. X. Huang, J. Liang, S. Rtimi, B. Devakumar, and Z. Zhang, "Ultra-high color rendering warm-white light-emitting diodes based on an efficient green-emitting garnet phosphor for solid-state lighting," Chem. Eng. J. **405**, 126950 (2021).
5. S. Wang, B. Devakumar, Q. Sun, J. Liang, L. Sun, and X. Huang, "Highly efficient near-UV-excitable $Ca_2YHf_2Al_3O_{12}$:Ce^{3+},Tb^{3+} green-emitting garnet phosphors with potential application in high color rendering warm-white LEDs," J. Mater. Chem. C **8**, 4408 (2020).
6. B. Shen, F. Wu, Y. Zhang, H. Xia, B. Chen, and J. Hu, "Multicolour emission from thermally stable Tb^{3+}/Eu^{3+} co-doped $CaLa_4Si_3O_{13}$ phosphors for single-component w-LEDs application," J. Alloys Compd. **809**, 151836 (2019).
7. S. Kaur, M. Jayasimhadri, and A. S. Rao, "A novel red emitting Eu^{3+} doped calcium aluminozincate phosphor for applications in w-LEDs," J. Alloys Compd. **697**, 367 (2017).
8. R. Cao, X. Lv, Y. Jiao, Y. Ran, S. Guo, H. Ao, T. Chen, and T. Fan, "$Ca_3La_6Si_6O_{24}$:Eu^{3+} orange-red-emitting phosphor: synthesis, structure and luminescence properties," Mater. Res. Bull. **122**, 110651 (2020).
9. L. Sun, B. Devakumar, J. Liang, S. Wang, Q. Sun, and X. Huang, "Highly efficient Ce^{3+} → Tb^{3+} energy transfer induced bright narrowband green emissions from garnet-type $Ca_2YZr_2(AlO_4)_3$:Ce^{3+},Tb^{3+} phosphors for white LEDs with high color rendering index," J. Mater. Chem. C **7**, 10471 (2019).
10. X. Huang, H. Guo, L. Sun, T. Sakthivel, and Y. Wu, "A high-efficiency, broadband-excited cyan-emitting $Ba_3Lu_2B_6O_{15}$:Ce^{3+},Tb^{3+} phosphor for near-UV-pumped white light-emitting diodes," J. Alloys Compd. **787**, 865 (2019).
11. X. Li, C. Yang, Q. Liu, X. Wang, and X. Mi, "Enhancement of luminescence properties of $SrAl_2Si_2O_8$: Eu^{3+} red phosphor," Ceram. Int. **46**, 17376 (2020).
12. X. Huang, H. Guo, and B. Li, "Eu^{3+}-activated $Na_2Gd(PO_4)(MoO_4)$: a novel high-brightness red-emitting phosphor with high color purity and quantum efficiency for white light-emitting diodes," J. Alloys Compd. **720**, 29 (2017).
13. X. Huang, B. Li, H. Guo, and D. Chen, "Molybdenum-doping-induced photoluminescence enhancement in Eu^{3+}-activated $CaWO_4$ red-emitting phosphors for white light-emitting diodes," Dyes Pigments **143**, 86 (2017).
14. X. Huang, S. Wang, B. Li, Q. Sun, and H. Guo, "High-brightness and high-color purity red-emitting $Ca_3Lu(AlO)_3(BO_3)_4$:Eu^{3+} phosphors with internal quantum efficiency close to unity for near-ultraviolet-based white-light-emitting diodes," Opt. Lett. **43**, 1307 (2018).
15. N. Ding, L. Zhang, Q. Liu, T. Xu, and Q. Zhang, "Luminescence properties of novel double perovskite Gd_2MgTiO_6:Eu^{3+} phosphors prepared by solid state method," J. Mater. Sci. Mater. Electron. **28**, 12239 (2017).
16. S. Kato, M. Ogasawara, M. Sugai, and S. Nakata, "Crystal structure and property of perovskite-type oxides containing ion vacancy," Catal. Surv. Asia **8**, 27 (2004).
17. R. D. Shannon, "Revised effective ionic radii and systematic studies of interatomic distances in halides and chaleogenidess," Acta Crystallogr. A **32**, 751 (1976).
18. G. Li, Y. Wei, Z. Li, and G. Xu, "Synthesis and photoluminescence of Eu^{3+} doped $CaGd_2(WO_4)_4$ novel red phosphors for white LEDs applications," Opt. Mater. **66**, 253 (2017).
19. J. Liang, P. Du, H. Guo, L. Sun, B. Li, and X. Huang, "High-efficiency and thermal-stable $Ca_3La(GaO)_3(BO_3)_4$:Eu^{3+} red phosphors excited by near-UV light for white LEDs," Dyes Pigments **157**, 40 (2018).
20. Q. Zhang, X. Wang, X. Ding, and Y. Wang, "A potential red-emitting phosphor $BaZrGe_3O_9$:Eu^{3+} for WLED and FED applications: synthesis, structure, and luminescence properties," Inorg. Chem. **56**, 6990 (2017).
21. D. Zhao, Y.-L. Xue, S.-R. Zhang, L.-Y. Shi, B.-Z. Liu, Y.-P. Fan, Q.-X. Yao, and S.-J. Dai, "Non-concentration quenching, good thermal stability and high quantum efficiency of $K_5Y(P_2O_7)_2$:Eu^{3+}/Tb^{3+} phosphors with a novel two-dimensional layer structure," J. Mater. Chem. C **7**, 14264 (2019).
22. G. Dong, J. Zhao, M. Li, L. Guan, and X. Li, "A novel red Y_2MoSiO_8:Eu^{3+} phosphor with high thermal stability for white LEDs," Ceram. Int. **45**, 2653 (2019).
23. D. Zhao, Y. Xue, R. Zhang, Y. Fan, B. Liu, Y. Li, and S. Zhang, "Design, synthesis, crystal structure and luminescent properties introduced by Eu^{3+} of a new type of rare-earth borophosphate $CsNa_2REE_2(BO_3)(PO_4)_2$ (REE = Y, Gd)," Dalton Trans. **49**, 10104 (2020).
24. L. Lakshmi Devi and C. K. Jayasankar, "Spectroscopic investigations on high efficiency deep red-emitting Ca_2SiO_4:Eu^{3+} phosphors synthesized from agricultural waste," Ceram. Int. **44**, 14063 (2018).
25. H. Guo, X. Huang, and Y. Zeng, "Synthesis and photoluminescence properties of novel highly thermal-stable red-emitting $Na_3Sc_2(PO_4)_3$:Eu^{3+} phosphors for UV-excited white-light-emitting diodes," J. Alloys Compd. **741**, 300 (2018).
26. C. Ji, T.-H. Huang, Z. Huang, J. Wen, W. Xie, X. Tian, T. Wu, H. He, and Y. Peng, "High thermal stability and colour saturation red-emitting $Ba_2AGe_2O_7$: Eu^{3+} (A = Mg, Zn) phosphors for WLEDs," J. Lumin. **216**, 116734 (2019).
27. S. Fang, T. Lang, T. Han, M. Cai, S. Cao, L. Peng, B. Liu, Y. Zhong, A. N. Yakovlev, and V. I. Korepanov, "A novel efficient single-phase dual-emission phosphor with high resemblance to the photosynthetic spectrum of chlorophyll A and B," J. Mater. Chem. C **8**, 6245 (2020).